Nuclear Engineering and Technology 48 (2016) 785–794

Available online at ScienceDirect

Nuclear Engineering and Technology

journal homepage: www.elsevier.com/locate/net

Original Article

Electron Accelerator Shielding Design of KIPT Neutron Source Facility

Zhaopeng Zhong * *and Yousry Gohar*

Argonne National Laboratory, 9700 South Cass Avenue, Argonne, IL 60439, USA

ARTICLE INFO

Article history:
Received 6 August 2015
Received in revised form
18 November 2015
Accepted 6 January 2016
Available online 27 January 2016

Keywords:
Electron Accelerator
Monte Carlo Simulation
Shield Design

ABSTRACT

The Argonne National Laboratory of the United States and the Kharkov Institute of Physics and Technology of the Ukraine have been collaborating on the design, development and construction of a neutron source facility at Kharkov Institute of Physics and Technology utilizing an electron-accelerator-driven subcritical assembly. The electron beam power is 100 kW using 100-MeV electrons. The facility was designed to perform basic and applied nuclear research, produce medical isotopes, and train nuclear specialists. The biological shield of the accelerator building was designed to reduce the biological dose to less than 5.0e-03 mSv/h during operation. The main source of the biological dose for the accelerator building is the photons and neutrons generated from different interactions of leaked electrons from the electron gun and the accelerator sections with the surrounding components and materials. The Monte Carlo N-particle extended code (MCNPX) was used for the shielding calculations because of its capability to perform electron-, photon-, and neutron-coupled transport simulations. The photon dose was tallied using the MCNPX calculation, starting with the leaked electrons. However, it is difficult to accurately tally the neutron dose directly from the leaked electrons. The neutron yield per electron from the interactions with the surrounding components is very small, ~0.01 neutron for 100-MeV electron and even smaller for lower-energy electrons. This causes difficulties for the Monte Carlo analyses and consumes tremendous computation resources for tallying the neutron dose outside the shield boundary with an acceptable accuracy. To avoid these difficulties, the SOURCE and TALLYX user subroutines of MCNPX were utilized for this study. The generated neutrons were banked, together with all related parameters, for a subsequent MCNPX calculation to obtain the neutron dose. The weight windows variance reduction technique was also utilized for both neutron and photon dose calculations. Two shielding materials, heavy concrete and ordinary concrete, were considered for the shield design. The main goal is to maintain the total dose outside the shield boundary less than 5.0e-03 mSv/h during operation. The shield configuration and parameters of the accelerator building were determined and are presented in this paper.

* *Corresponding author.*
E-mail address: zzhong@anl.gov (Z. Zhong).

http://dx.doi.org/10.1016/j.net.2016.01.004

1. Introduction

Accelerator driven systems are under consideration for fuel cycle scenarios of light-water power reactors intended for closing the fuel cycle by transmuting actinides and long-lived fission products. Several studies have been performed using accelerator-driven subcritical systems. The Argonne National Laboratory and the National Science Center-Kharkov Institute of Physics and Technology (KIPT) have been collaborating on developing and constructing a neutron source facility at KIPT that uses an electron-accelerator-driven subcritical assembly [1]. The facility has been constructed and is currently being commissioned. The main functions of this facility are medical isotope production and support of the Ukraine nuclear industry. Also, accelerator-driven systems physics experiments and material research will be carried out. The neutron source facility is driven by a linear electron accelerator with 100-kW electron beam power using 100-MeV electrons. The total length of the electron accelerator building is ~30 m, and the building can be divided into two parts for the shielding analyses. The first part contains the electron gun and the first accelerator section. This section has high electron losses but the electron energy is relatively low. The second part includes the remainder of the accelerator sections and has much lower electron loss but the electron energy is higher, up to 100 MeV. The leaked electrons generate photons and neutrons from their interactions with the surrounding components and materials. Therefore a biological shield is used in all the accelerator components.

The shielding study defined the radiation dose outside the shield boundary of the accelerator building as a function of the shield thickness. The main objective is to reduce the biological dose to permit personnel to work outside the accelerator building during operation. The shield design was configured to reduce the biological dose to less than 5.0e-03 mSv/h. This value is a factor of five less than the international standard of 2.5e-02 mSv/h for occupational limit, assuming 40 hours per week and 50 weeks per year.

The shielding analyses require accurate characterization of the neutron and photon fluxes through the shield. The Monte Carlo N-particle extended code MCNPX [2] has been widely used in the shielding analyses of accelerator applications [3–5], due to its updated capability for coupled charged particles, neutron, and photon transport calculations. For this study, MCNPX was also used with ENDF/B-VII.0 [6] nuclear data libraries for performing the shielding analyses. Both heavy concrete (4.8 g/cm^3) and ordinary concrete (2.3 g/cm^3) were considered for the biological shield study in order to define the required thickness from each type of concrete. Because direct analog calculation of the neutron and photon fluxes is impractical due to the excessive required computation resources, variance-reduction techniques were used to obtain accurate analyses with reasonable computational resources. Mesh-based weight windows were utilized for generating a space and energy-dependent importance function for the dose tally. Due to the low neutron yield per electron, the neutron source procedure [7–9] was utilized for accurate calculation of neutron fluxes outside the shield boundary. The SOURCE [2] and TALLYX [2] user subroutines of MCNPX were employed for the shielding analyses.

2. Materials and methods

2.1. *Electron beam loss in the acceleration tunnel*

Electron beam loss data were obtained from the accelerator design analyses. Most beam losses occur at the first accelerator section where the electrons are accelerated to less than 15 MeV. Losses in the rest of the accelerator sections are relatively low. The electron energy increases from less than 1 MeV to 100 MeV along the accelerator sections as shown in Fig. 1 and the corresponding electron losses are shown in Fig. 2. The total power of the lost electrons shown in Fig. 2 is ~2.84 kW and is distributed unevenly along the electron beam axis Z. The biggest electron beam loss occurs at Z equal to ~500 cm where electron energy is ~12.4 MeV as shown in Fig. 2. At this location, the electron beam loss is at ~1.27 kW. After this location, the electron energy increases up to 100 MeV, and

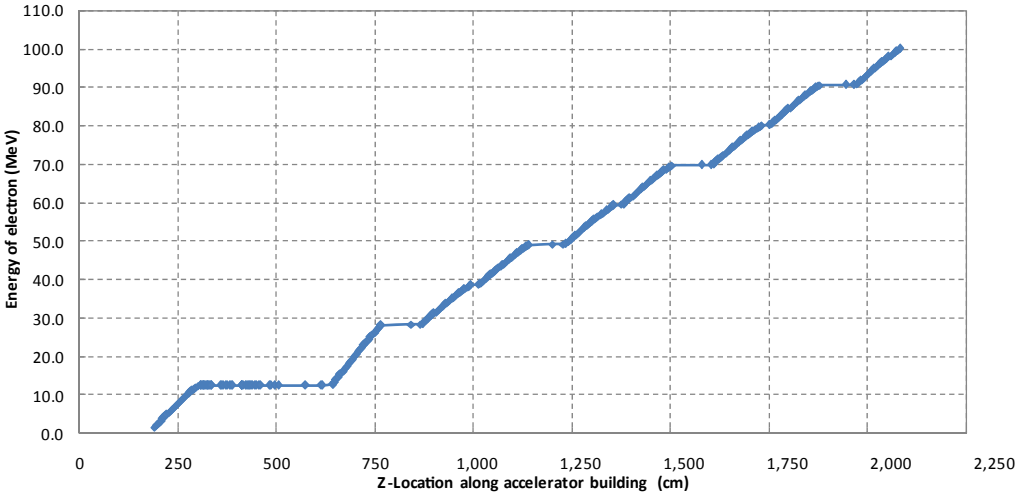

Fig. 1 – Electron energy along the acceleration building.

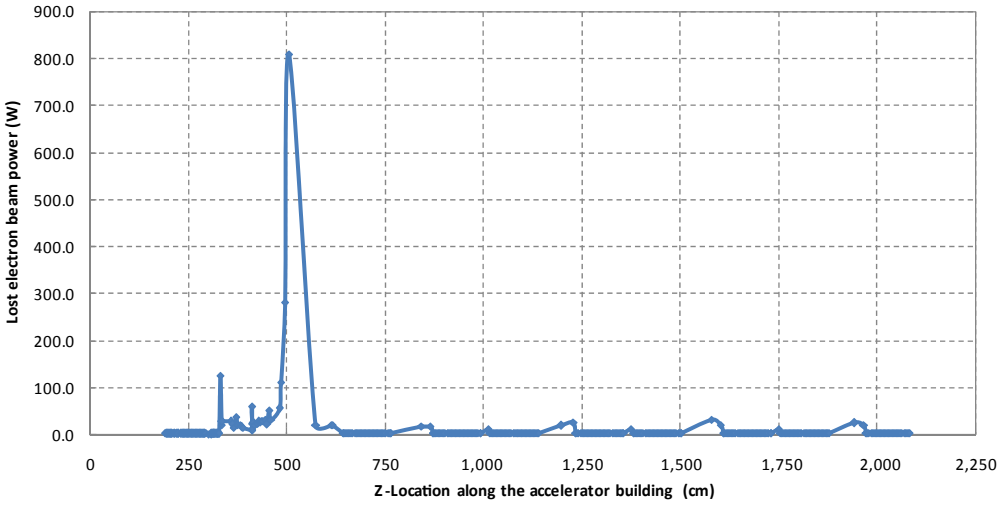

Fig. 2 – Electron beam power losses along the acceleration building.

the electron beam losses are trivial except for few local small peaks, as shown in Fig. 2. When the electron energy reaches 100 MeV, the beam losses in the end section of the accelerator building have a uniform distribution of ~50 W/m (not shown in Fig. 2). Although beam losses beyond the first accelerator section are relatively lower than those of the first section, they produce significant photon and neutron doses because of the higher electron energy. Therefore, the shield analyses considered all the losses along the length of the whole accelerator building.

2.2. *Calculation model*

The electron beam tube is made of 2-mm-thick stainless steel. The accelerator building has a rectangular cross-section. Dimensions from the beam center to the left, right, top, and bottom walls are 1.5 m, 1.5 m, 1.3 m, and 1.2 m, respectively, as shown in Fig. 3. To improve computational efficiency, a cylindrical geometry was used for the MCNPX model as shown Fig. 4. The inner radius of the shielding wall is set at 1.2 m—the minimal distance between the beam tube center and the wall surface. The electron emission angle is 10° relative to the beam direction. In any plane perpendicular to the electron beam tube, the lost electrons have a uniform azimuthal distribution. Therefore, an annular tally was utilized for the MCNPX calculation utilizing the cylindrical geometry to reduce statistical errors in the tallied results. This MCNPX model is conservative with respect to the biological dose value outside the shield boundary. With the same shield thickness, the average dose on the external shield surface of the cylindrical model would be the peak dose for the real geometry model (on the external side of the bottom shield as shown in Fig. 3).

Due to the long length of the accelerator building (~30 m) and uneven distribution of the electron beam losses, the MCNPX calculation for the whole accelerator building is time consuming, considering the iterative calculation process needed to generate weight windows and determine the shield parameters. To use reasonable computer resources and to improve the MCNPX sampling efficiency for the lost high-energy electrons whose fraction is very small, two MCNPX models with smaller geometry were introduced, representing the beginning and end sections of the accelerator building where the largest biological dose values are expected. Due to the 10°-emission angle and the 1.2-m distance between the shielding wall and beam axis, the lost electrons would travel ~6.8 m along the beam axis before hitting the shielding wall, assuming there is no collision within the accelerator components. Therefore, the models should have sufficient length to let the lost electrons projecting on the shielding wall. The length is set to ~10 m for these two models. The first model (corresponding to the end section) has uniform beam losses of 50 W/m along the electron beam in the length of 10 m, and the beam energy is set to 100 MeV, as shown on left side of Fig. 5. The second model (corresponding to the beginning section) focuses on the biggest electron loss peak shown in Fig. 2, and it is simulated as a point electron source as shown on the right side of Fig. 5. Source strength is 1.27 kW, using 12.4-MeV

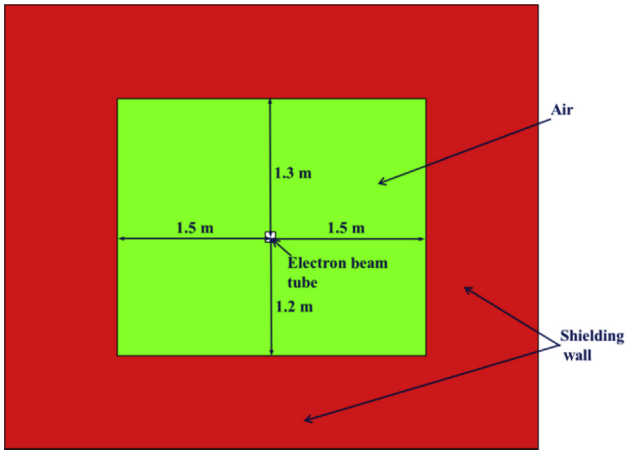

Fig. 3 – Cross section of accelerator building perpendicular to electron beam tube.

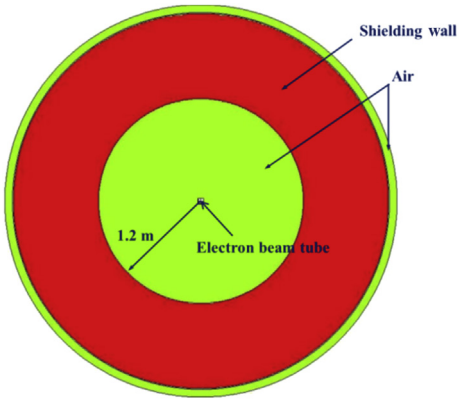

Fig. 4 – Cross section of MCNPX geometrical model of accelerator building perpendicular to electron beam tube.

electrons. This model produces a conservative shield design for the first section of the accelerator building.

The accelerator building is ~30 m long, which dictates the use of inexpensive shielding materials to avoid unreasonable cost. Ordinary concrete (2.3 g/cm^3) is a lower-cost shielding material than heavy concrete (4.8 g/cm^3) [10, 11]. The heavy concrete is an efficient shielding material for both neutrons and photons because it has a balanced mixture of light and heavy elements. It is more expensive than ordinary concrete because it has a high proportion of heavy elements in the form of steel shots, which slows the high-energy ($E > 10$ MeV) neutrons to the intermediate energy range by inelastic scattering. The high-energy neutrons generated by the 100-MeV electrons via photonuclear reactions dominate the biological dose outside the shield boundary, as shown in the shielding analyses of the subcritical assembly [7, 8]. In addition, heavy concrete has a high proportion of light elements that slows the intermediate energy neutrons to thermal neutrons for absorption within the heavy concrete. Although ordinary concrete is cheaper than heavy concrete, its shielding performance for neutrons and photons is inefficient due to the absence of heavy elements. Therefore much thicker concrete than heavy concrete would be required to reduce the biological radiation dose to an acceptable level, which also reduces the cost.

As mentioned earlier, the neutron and photon radiation dose profiles through the shield were obtained from separate MCNPX calculations. The photon dose was obtained from an MCNPX calculation starting with the electron source, while the neutron dose was calculated by a separate MCNPX calculation starting from the volumetric neutron source. The neutron source file is generated by a separate MCNPX calculation starting from electron particle. All the neutrons generated through photonuclear reactions in the accelerator components are recorded. This neutron source file recorded the position, energy, weight, and cosine directions of every born neutron. The TALLYX user subroutine of MCNPX was utilized to generate the volumetric neutron source file. The SOURCE subroutine was used to read the external neutron source file generated in the previous step to start a neutron transport calculation. Each record in the neutron source file could be used multiple times to reduce the statistic error. The weight windows variance reduction technique [12] of MCNPX was utilized in this study. Mesh-based weight windows were

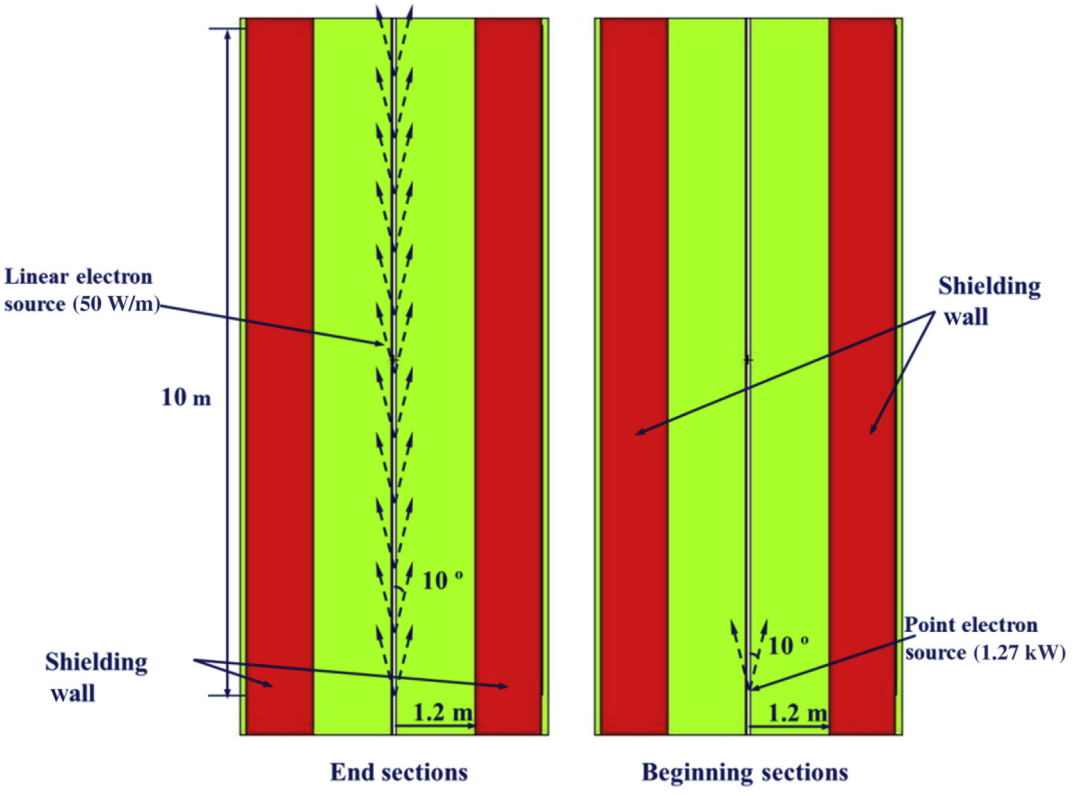

Fig. 5 – Axial configuration for the simplified MCNPX models of shielding wall for the accelerator building.

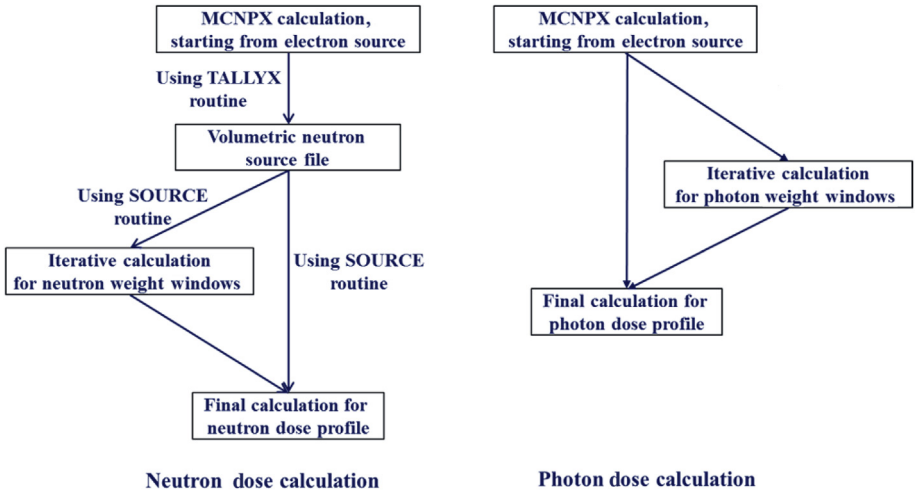

Fig. 6 – MCNPX calculation process for neutron- and photon-dose profiles.

generated using iterative MCNPX calculations [9] for both neutrons and photons. The calculation process of MCNPX for neutron and photon dose profiles is summarized in Fig. 6. Modified TALLYX and SOURCE user subroutines are needed in the neutron-dose calculation, while standard MCNPX calculates the photon dose.

3. Results

A series of iterative MCNPX calculations were used to determine the shield design. The two MCNPX calculation models, described in previous sections (see Figs. 4 and 5), were used to determine the shield thickness required to limit the biological dose to less than 5.0e-03 mSv/h. Firstly, an initial guess of the shield thickness was used to obtain the total dose (neutron and photon) distribution along the shield boundary. Then the shield thickness was revised based on the obtained results to keep the maximum dose value outside the shield boundary to less than 5.0e-03 mSv/h. The neutron and photon biological doses were obtained by using International Commission on Radiological Protection-21 (1971) [13] flux-to-dose conversion tables of MCNPX. After several iterative MCNPX calculations, the final shield thicknesses were determined.

Using the first MCNPX model representing the end section of accelerator building, neutron and photon radiation dose profiles were calculated using the mesh tally capability of MCNPX with heavy concrete as shielding material (as shown in Fig. 7), and with ordinary concrete as shielding material (as shown in Fig. 8). The x axis corresponds to the radius from the building center, while the y axis corresponds to the length along the electron beam. The mesh size for the tally is 10 cm in both x and y directions. Electron losses are distributed evenly along the y axis, from 0–1,000 cm with a 10° emission angle, and the electron energy is 100 MeV. In the dose map plots, the dashed line corresponds to the inner shield surface and the solid line corresponds to the outer shield surface. The outer shield radius is 2.2 m and 3.1 m for heavy concrete and ordinary concrete, respectively.

For heavy concrete, the 5.0e-03 mSv/h neutron dose contour line coincides with the outer shield surface, while the 5.0e-03 mSv/h photon dose contour line is 10–20 cm inside the shield, away from the shield boundary. In this case, the neutron dose determines the required shield thickness because it is much higher than the photon dose at the boundary. The ordinary concrete requires a 3.1-m outer shield radius, compared with 2.2 m for heavy concrete. As shown in Fig. 7, the 5.0e-03 mSv/h neutron dose contour line is 40–60 cm inside the shield away from the shield boundary, while the 5.0e-03 mSv/h photon dose contour line is close or coincides with the outer shield boundary. In this case, the photon dose determines the required shield thickness. This situation is expected for the ordinary concrete since it does not attenuate photons efficiently due to the absence of heavy elements. As seen in Fig. 8, the space between photon dose contour lines is ~20 cm in the inner side of shield but ~50 cm in the external side of shield. This difference is caused by the change of energy spectrum because the inner side consists of a large component of low-energy photons while in the external side the low energy photons are absorbed and only high-energy photons are left.

The total biological dose, neutron, and photon doses are also less than 5.0e-03 mSv/h outside the shield as shown in Figs. 9 and 10 for heavy concrete and ordinary concrete, respectively. The 5.0e-03 mSv/h total dose contour line is still within the shield boundary for the two shield options. The results of Figs. 8 and 9 show that the 5.0e-03 mSv/h contour line is away from the outer shield surface for $y < 4$ m because of the 10° emission angle of the lost electron relative to the electron beam axis. The total biological dose along the outer shield boundary has a statistical error of less than 1% for the regions with the large dose values for $y > 4$ m.

The second MCNPX model representing the beginning section of accelerator building, the lost electron energy is 12.4 MeV and the neutron yield from different interactions of these electrons is insignificant. Therefore, the biological dose from the generated neutrons is negligible. In this case, the

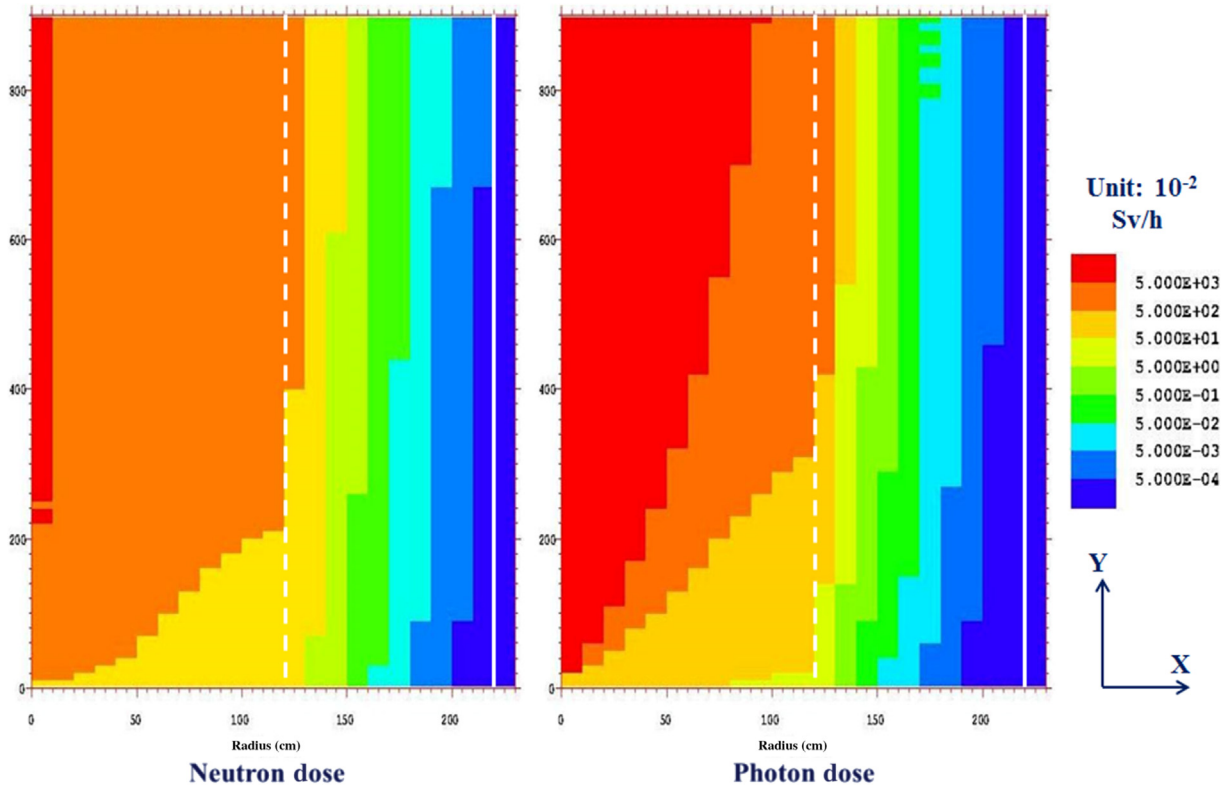

Fig. 7 – Neutron and photon dose profile in the end section of accelerator building with heavy concrete shielding material.

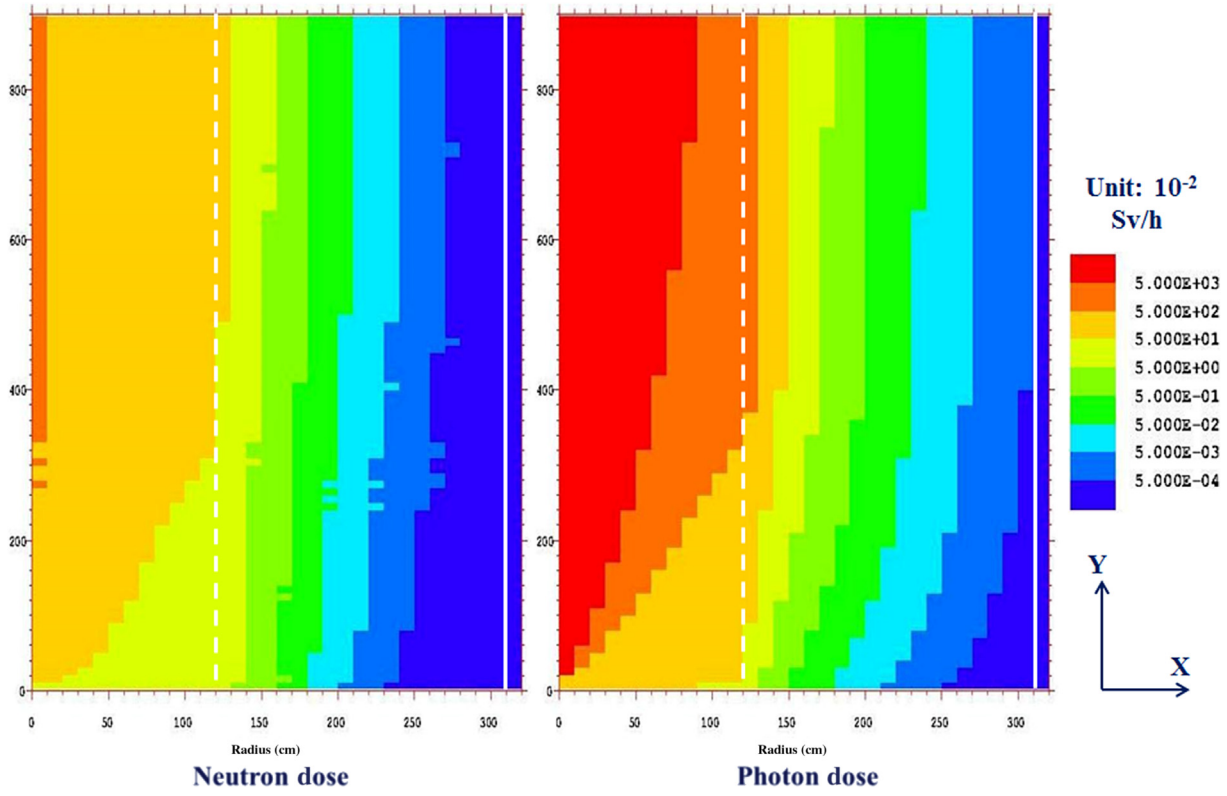

Fig. 8 – Neutron and photon dose profile in the end section of accelerator building with ordinary concrete shielding material.

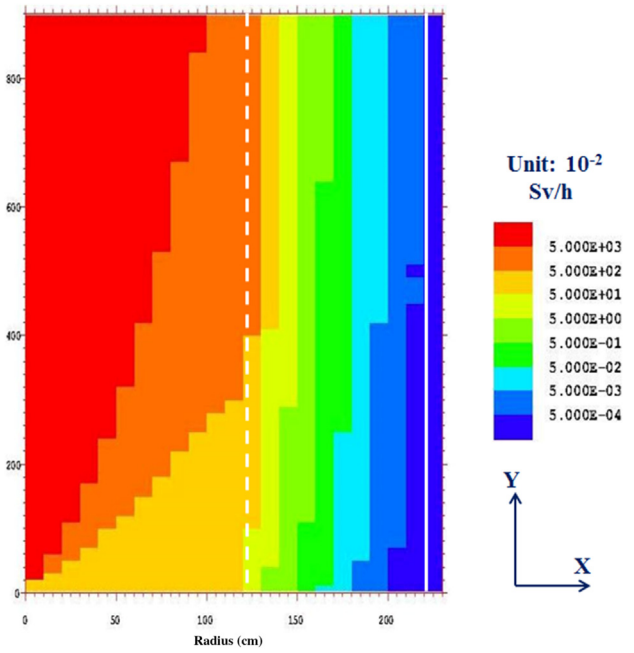

Fig. 9 – Total dose profile in the end section of accelerator building with heavy concrete shielding material.

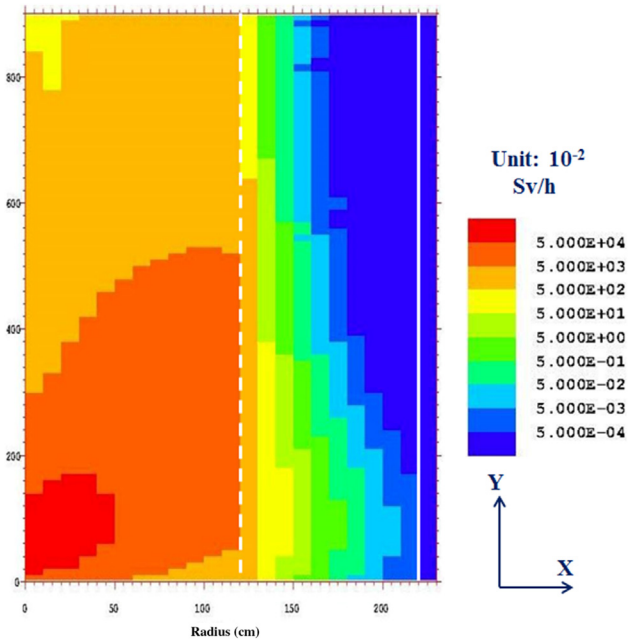

Fig. 11 – Photon dose profile in the beginning section of accelerator building with heavy concrete shielding material.

biological dose from the generated photons defines the required shield thickness. Photon dose profiles were calculated using the mesh tally capability of MCNPX and the results are shown in Figs. 11 and 12 for heavy concrete and ordinary concrete, respectively. Again, the x axis corresponds to the radius from the electron beam center, and the y axis corresponds to the length along the electron beam direction. The mesh size for the tally is uniformly 10 × 10 cm. The point electron source is located at x = 0 and y = 0. The dashed line corresponds to the inner shield boundary and the solid line corresponds to the outer shield boundary. The outer shield radius is 2.2 m and 3.4 m for heavy concrete and ordinary concrete, respectively. For both cases, the 5.0e-03 mSv/h photon dose contour line is within or coinciding with the outer shield boundary.

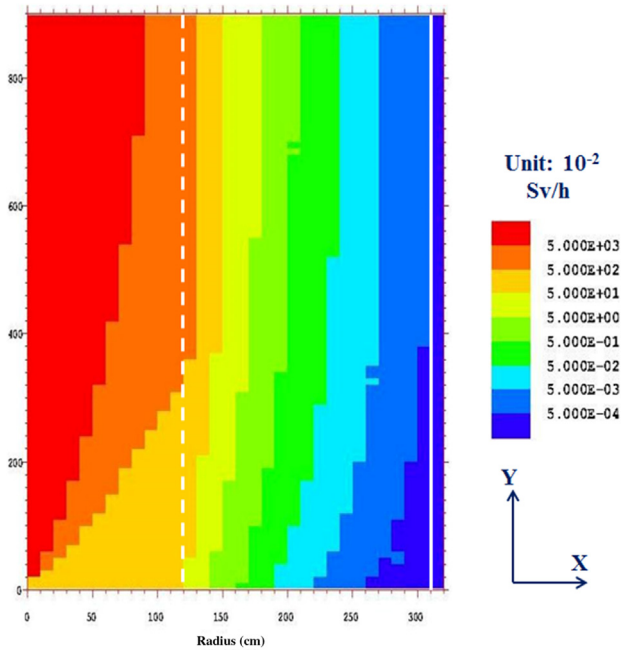

Fig. 10 – Total dose profile in the end section of accelerator building with ordinary concrete shielding material.

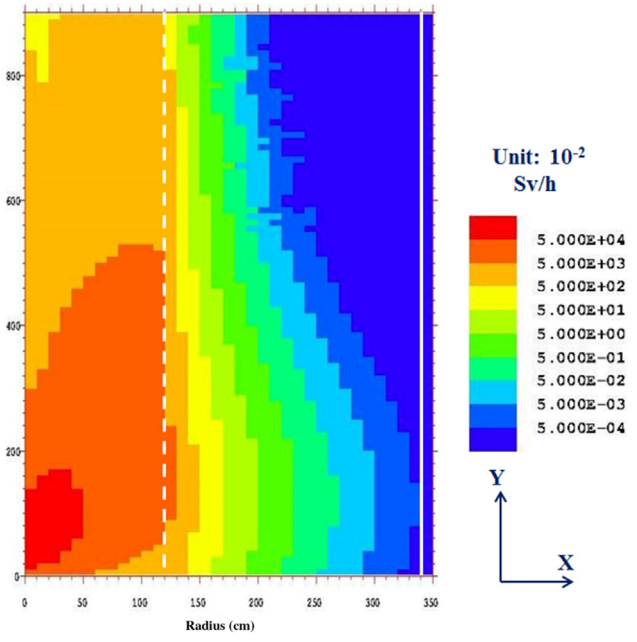

Fig. 12 – Photon dose profile in the beginning section of accelerator building with normal concrete shielding material.

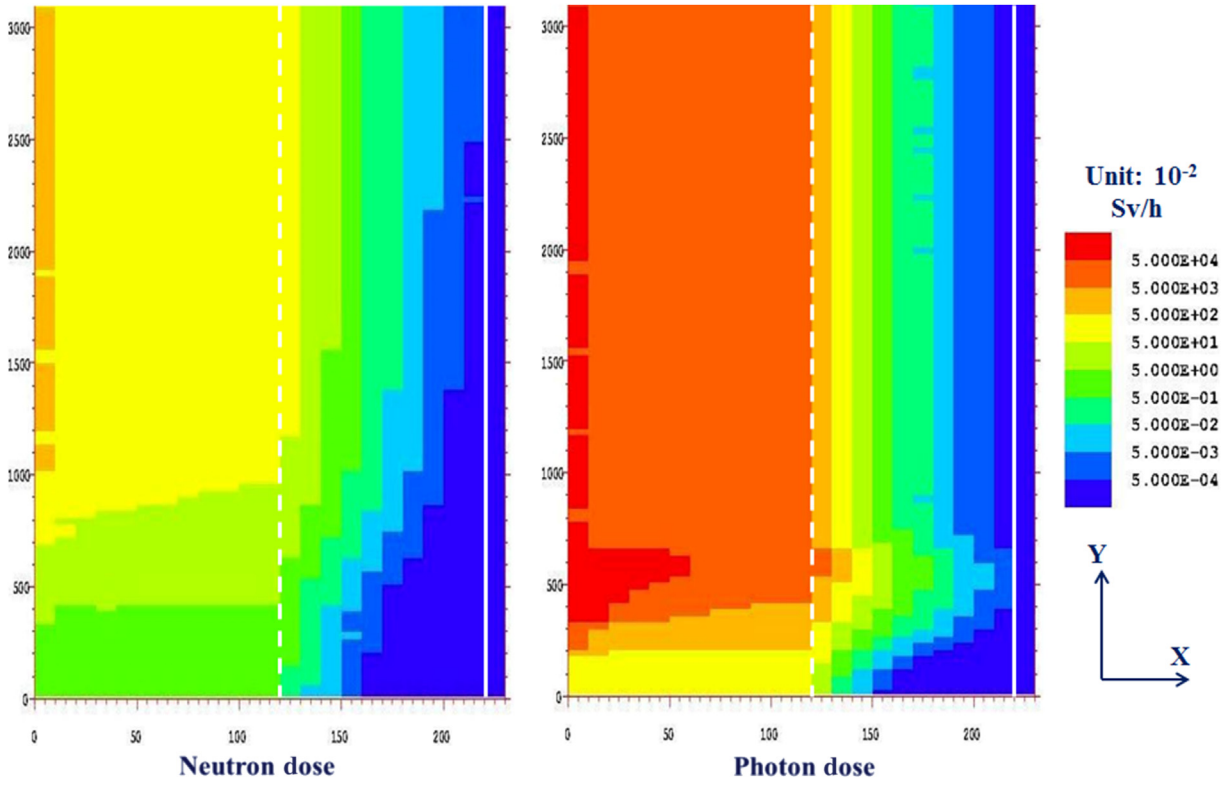

Fig. 13 – Neutron and photon dose profile along the whole accelerator building with heavy concrete shield material.

Although the lost electrons have a 10° emission angle relative to the electron beam axis (y axis), the peak photon dose at the outer shield boundary occurs at y = 1 m as shown in Figs. 11 and 12. This result differs from the previous analyses for the high-energy electrons. The 2-mm-thick stainless steel beam tube material is almost transparent for the 100-MeV electrons, and these electrons reach the inner shield boundary before any significant interaction with the beam tube. On the contrary, the 12.4-MeV electrons interact with the beam tube and generate a significant number of photons. The maximum photon dose value at the outer shield boundary has less than 1% statistical error. The required ordinary concrete thickness is 30 cm greater than the end section of the accelerator building, because of the high photon source intensity as well as the low photon attenuation capability of the ordinary concrete.

The results show that the required heavy concrete shield thickness is 1.0 m for both the first and end sections of the accelerator building. For the ordinary concrete option, the required thicknesses are 1.9 m and 2.2 m for the end and the first sections of the accelerator building, respectively.

Based on the results and comparing the required shield volume for normal and heavy concretes, the ratio is ~2.3 and 2.9 for the end and the first sections of the accelerator building. Considering the space limitation inside and outside the facility building, heavy concrete was selected as the shielding material. In addition, the shield thickness is the same for both the first and end sections of the accelerator building, which simplifies the accelerator building design.

The heavy concrete shield thickness was determined to be 1.0 m based on the previous calculations and analyses. However, the two simplified MCNPX models used previously represent only the first and end sections of the accelerator building. The electron beam losses in the other sections of the accelerator building, especially the small peaks at Z from 750 cm to 2,000 cm (Fig. 2), could generate local high biological dose areas. To confirm, the 1.0-m heavy-concrete shield thickness is sufficient to keep the radiation dose outside the shield boundary less than 5.0e-03 mSv/h, another MCNPX model was developed to validate the shield design using the electron beam losses along the whole accelerator building. The lost electrons still have a 10° emission angle and are evenly distributed azimuthally. The SOURCE subroutine of MCNPX was modified to model the electron source with the exact energy and spatial distribution (Figs. 1 and 2). The electron beam loss in the end section of the accelerator building, with electron energy 100 MeV and strength 50 W/m, is also modeled by the SOURCE subroutine. The geometry is still cylindrical, with an inner radius of 1.2 m and an outer radius of 2.2 m. The neutron and photon doses are calculated by separate MCNPX runs, with neutron source file generated and utilized in neutron dose calculation, while photon dose calculation starts from electron source directly. Weight windows variance reduction technique is also utilized in both neutron and photon dose calculation. The neutron and photon radiation dose profiles have been calculated using the mesh tally capability of MCNPX (Fig. 13). The x axis corresponds to the radius in cm from the tunnel center, while the y axis corresponds to the length in centimeters along the electron beam tunnel. The length of the MCNPX model is ~30 m, and the values of the y axis are consistent with those of the z axis of Figs. 1 and 2. For the mesh tally, the mesh dimension in the x direction was still 10 cm but it was

increased to 30 cm in the y direction. The dashed line corresponds to the inner shield boundary and the solid line corresponds to the outer shield boundary.

Fig. 13 shows that the neutron dose through the shield for $y < 14$ m is very low due to the lower energy of the lost electrons and smaller neutron yield in the range. While the neutron dose increases along the y axis for $y > 14$ m. The 5.0e-03 mSv/h neutron dose contour line is 10 cm away from the outer shield boundary. This is because the higher energy of the lost electrons increases the neutron yield, despite the smaller intensity of electron loss. The photon dose peak through the shield appears at y ~5 m, which matches approximately the location of the biggest electron loss, and these results are consistent with the results shown in Fig. 10. The photon dose peak is due to the interaction of the lost electrons with 2-mm thick electron beam tube. The 5.0e-03 mSv/h photon dose contour line is ~10 cm away from the outer shield boundary.

The total radiation dose map through the whole accelerator building is plotted in Fig. 14, where the 5.0e-03 mSv/h contour line is consistently within the outer shield. The statistical error for the results shown in Fig. 13 is larger than those for Figs. 8 and 10 because of the large size of calculation model. However, the statistical error of the total dose on the outer shield surface is still less than 10 % for the region with $y > 3$ m. The results shown in Fig. 14 mean the 1.0-m thick heavy concrete shield satisfies the shield design requirement.

4. Discussion

The Monte Carlo computer code (MCNPX) was utilized to determine the shield design of the accelerator building of the KIPT neutron source facility of Ukraine. The neutron and photon doses were analyzed using separate MCNPX calculations to reduce the statistical error in the results and to use reasonable computer resources. A neutron source file was developed and utilized to calculate the neutron dose map, while the photon dose map was obtained from MCNPX calculation starting directly with the electron source. The weight windows variance reduction technique was used for both the neutron and photon dose calculations; this was essential in these analyses to reduce statistical errors. Conservative cylindrical geometrical models were developed to further reduce statistical errors in the dose results. Both heavy concrete and ordinary concrete shield options were considered. For the end section of the accelerator building with 50 W/m uniform electron beam losses and electron energy of 100 MeV, the required shield thickness is 1.0 m and 1.9 m for heavy concrete and ordinary concrete, respectively, if the total dose outside the shield boundary is kept less than 5.0e-03 mSv/h along the outer shield boundary. For the first section of the accelerator building with high beam power losses with 12.4 MeV electrons, the corresponding shield thickness is 1.0 m and 2.2 m for heavy and ordinary concrete, respectively.

Heavy concrete was selected as the shielding material to minimize the shield footprint, especially in the subcritical assembly experimental hall. Using the heavy concrete shield with uniform 1.0-m thickness. A full MCNPX model of the facility with 1-m heavy concrete shield was developed to verify the shield design. The results from this model confirm that the 5.0e-03 mSv/h total dose contour line is consistently within or coincides with the outer shield boundary. This indicates that the electron loss in the middle sections will not introduce unacceptable radiation outside the shield boundary and the 1.0-m heavy-concrete shield thickness is sufficient for the whole accelerator building.

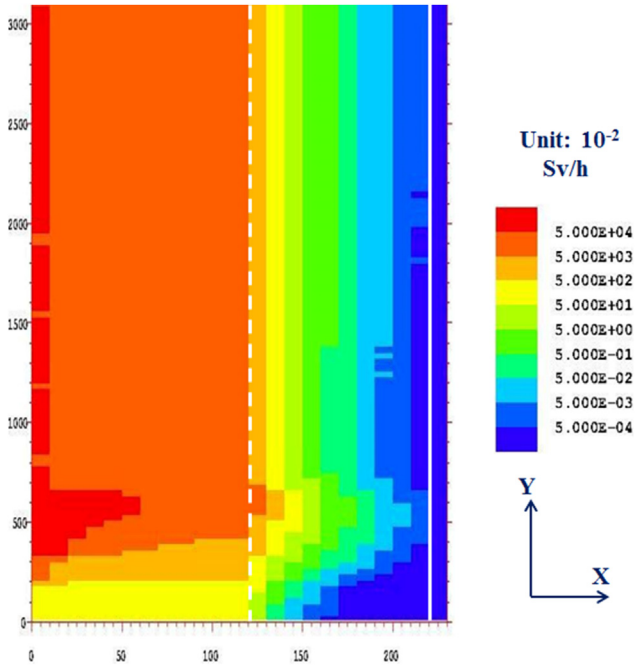

Fig. 14 – Total biological dose map, neutrons, and photons, along the acceleration tunnel with heavy concrete shield material.

Conflicts of interest

All authors have no conflicts of interest to declare.

Acknowledgments

This work is supported by the U.S. Department of Energy, Office of Material Management and Minimization (M3), National Nuclear Security Administration.

REFERENCES

[1] Y. Gohar, I. Bolshinsky, D. Naberezhnev, Accelerator-driven sub-critical facility: conceptual design development, Nucl. Instr. Meth. Phys. Res. A 562 (2006) 870–874.
[2] Denise B. Pelowitz, John S. Hendricks, et al., MCNPX.2.7.B Extension, Los Alamos National Laboratory, 2009. LA-UR-09–04150.
[3] Y.O. Lee, Y.S. Cho, Y.J. Chang, Shielding Aspect of High Current Proton Linear Accelerator (KOMAC), Proceedings of the Korean Nuclear Society Autumn Meeting, Yongpyong (Korea), 2003.

[4] Y.S. Min, C.W. Lee, K.J. Mun, J. Nam, J.Y. Kim, Shielding design for the target room of the Proton Accelerator Research Center, J. Korean Phys. Soc. 56 (2010) 1971.
[5] S. Ohnishi, S. Maebara, Y. Sakaki, S. Sato, K. Ochiai, C. Konno, Radiation shielding design for IFMIF/EVEDA accelerator vault, J. Plasma Fusion Res. 9 (2010) 190–192.
[6] M.B. Chadwick, P. Obložinský, M. Herman, N.M. Greene, R.D. McKnight, D.L. Smith, P.G. Young, R.E. MacFarlane, G.M. Hale, S.C. Frankle, A.C. Kahler, T. Kawano, R.C. Little, D.G. Madland, P. Moller, R.D. Mosteller, P.R. Page, P. Talou, H. Trellue, M.C. White, W.B. Wilson, R. Arcilla, C.L. Dunford, S.F. Mughabghab, B. Pritychenko, D. Rochman, A.A. Sonzogni, C.R. Lubitz, T.H. Trumbull, J.P. Weinman, D.A. Brown, D.E. Cullen, D.P. Heinrichs, D.P. McNabb, H. Derrien, M.E. Dunn, N.M. Larson, L.C. Leal, A.D. Carlson, R.C. Block, J.B. Briggs, E.T. Cheng, H.C. Huria, M.L. Zerkle, K.S. Kozier, A. Courcelle, V. Pronyaev, S.C. van der Marck, ENDF/B-VII.0: next generation evaluated nuclear data library for nuclear science and technology [Internet]. Nucl. Data Sheets 107 (2006) 2932–3061. Available from: http://www.nndc.bnl.gov/endf/b7.0/.
[7] Z. Zhong, Y. Gohar, Shielding design and analysis of KIPT neutron source facility, Prog. Nucl. Energ. 53 (2011) 92.
[8] Z. Zhong, Y. Gohar, Neutron Source in the MCNPX Shielding Calculation for Electron Driven Facility, Physor 2012, Advances in Reactor Physics, Knoxville (TN), 2012.
[9] Z. Zhong, Y. Gohar, Biological shield design and analysis of KIPT accelerator driven-subcritical facility, Nucl. Technol. 168 (2009) 871.
[10] R.G. Williams, C.J. Gesh, R.T. Pagh, Compendium of Material Composition Data for Radiation Transport Modeling, PNNL-15870, Pacific North National Laboratory, 2006.
[11] R.L. Walker, A Summary of Shielding Constant for Concrete, ANL-6443, Argonne National Laboratory, 1961.
[12] C.N. Culbertson, J.S. Hendricks, An Assessment of the MCNP4C Weight Window, LA-13668, Los Alamos National Laboratory, 1999.
[13] International Commission on Radiological Protection, Conversion Coefficients for Use in Radiological Protection Against External Radiation, ICRP Publication 74, Ann. ICRP 26/3-4, 1996.